Supplementary Information

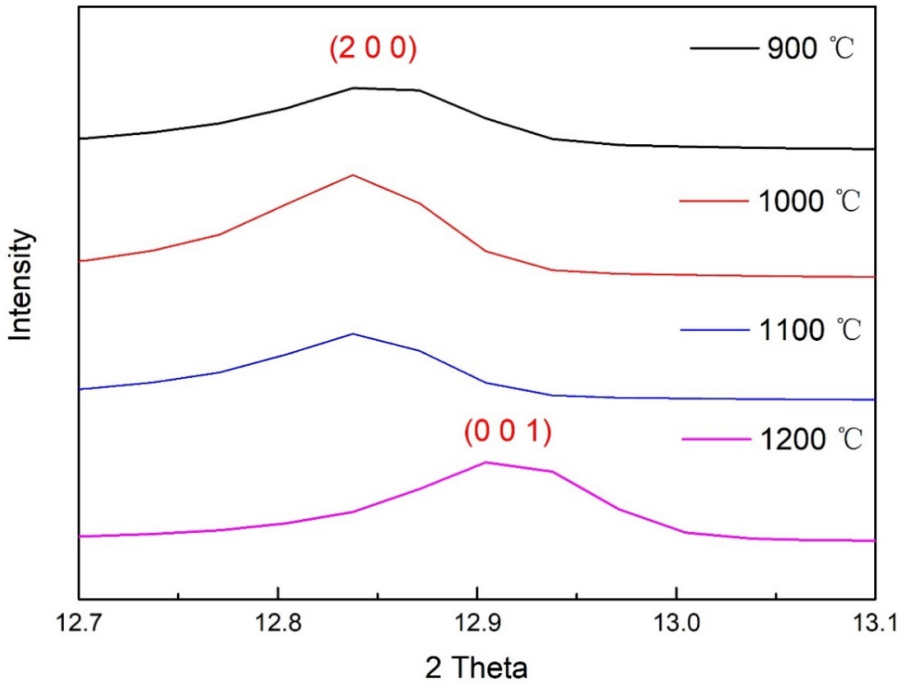

Figure S1. XRD patterns of MoO_3/MoS_2@G-900, MoO_3/MoS_2 @G-1000, MoO_3/MoS_2@G-1100 and MoO_3/MoS_2@G-1200 around the (2 0 0) reflection of orthorhombic MoO_3, and the (0 0 1) reflection of monoclinic MoO_3.

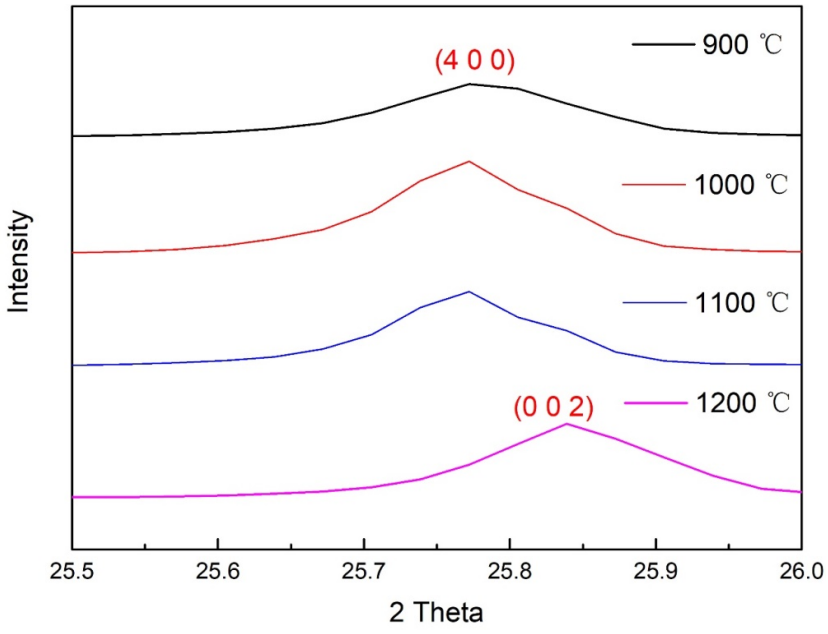

Figure S2. XRD pattern of MoO_3/MoS_2@G-900, MoO_3/MoS_2@G-1000, MoO_3/MoS_2@G-1100 and MoO_3/MoS_2@G-1200, around the (4 0 0) reflection of orthorhombic MoO_3, and the (0 0 2) reflection of monoclinic MoO_3.

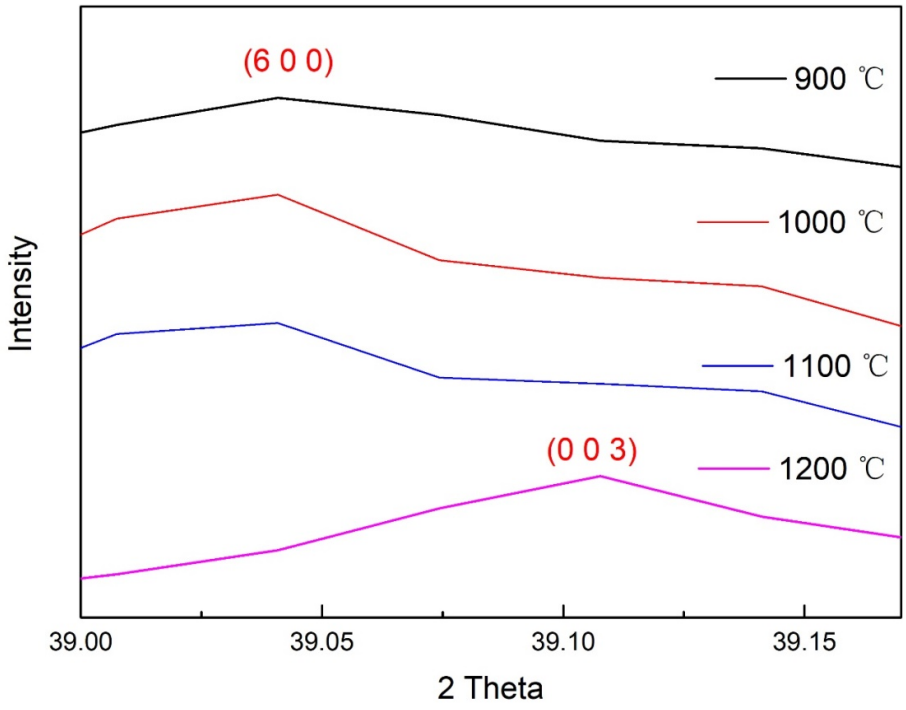

Figure S3. XRD patterns of MoO_3/MoS_2@G-900, MoO_3/MoS_2@G-1000, MoO_3/MoS_2@G-1100 and MoO_3/MoS_2@G-1200, around the (6 0 0) reflection of orthorhombic MoO_3, and the (0 0 3) reflection of monoclinic MoO_3.

Table S1. XRD peak intensity ratio corresponding to various peaks in MoO_3/MoS_2@G-900, MoO_3/MoS_2@G-1000, MoO_3/MoS_2@G-1100 and MoO_3/MoS_2@G-1200.

	Orthorhombic α-MoO_3 (200)/ MoS_2 (002)	**Orthorhombic α-MoO_3 (400)/C (002)**	**Orthorhombic α-MoO_3 (600)/ MoS_2 (103)**
MoO_3/MoS_2@G-900	1.34	1.04	6.37
MoO_3/MoS_2@G-1000	2.56	1.42	7.81
MoO_3/MoS_2@G-1100	3.30	1.92	8.27
	Monoclinic β- MoO_3 (0,0,1)/ MoS_2 (0,0,2)	Monoclinic β- MoO_3 (0,0,2)/C (0,0,2)	Monoclinic β- MoO_3 (0,0,3)/ MoS_2 (1,0,3)
MoO_3/MoS_2@G-1200	1.02	1.03	4.99

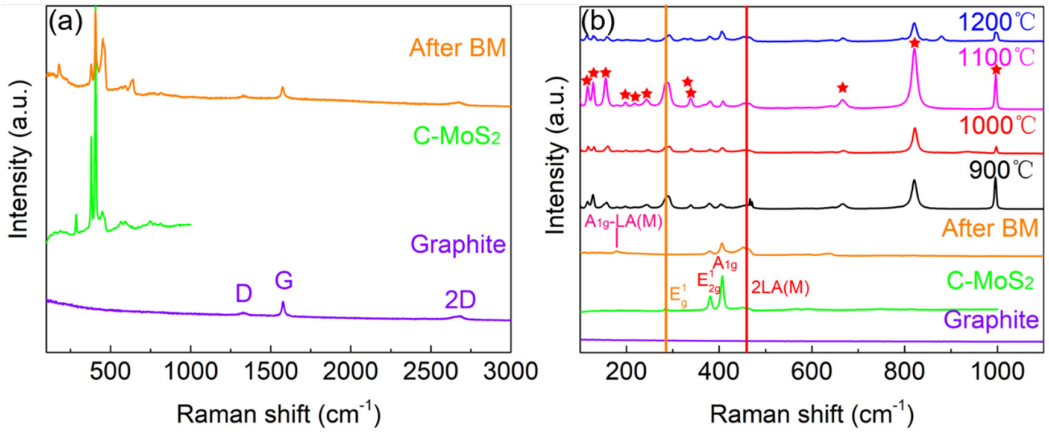

Figure S4. Raman spectra of various precursor materials and products obtained at various temperatures.

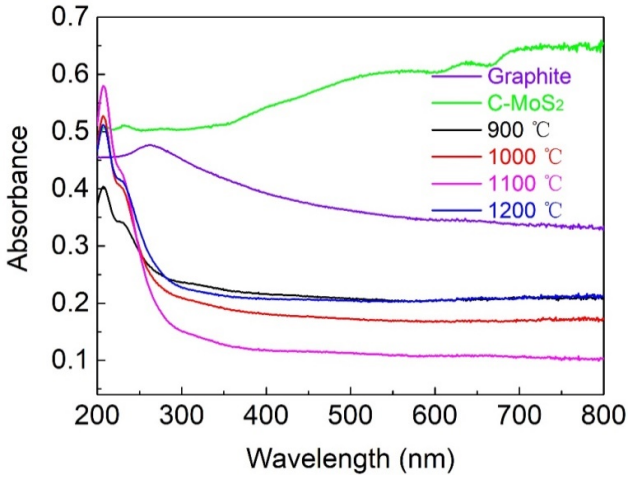

Figure S5. UV-vis spectra of various precursor materials and products obtained at various temperatures.

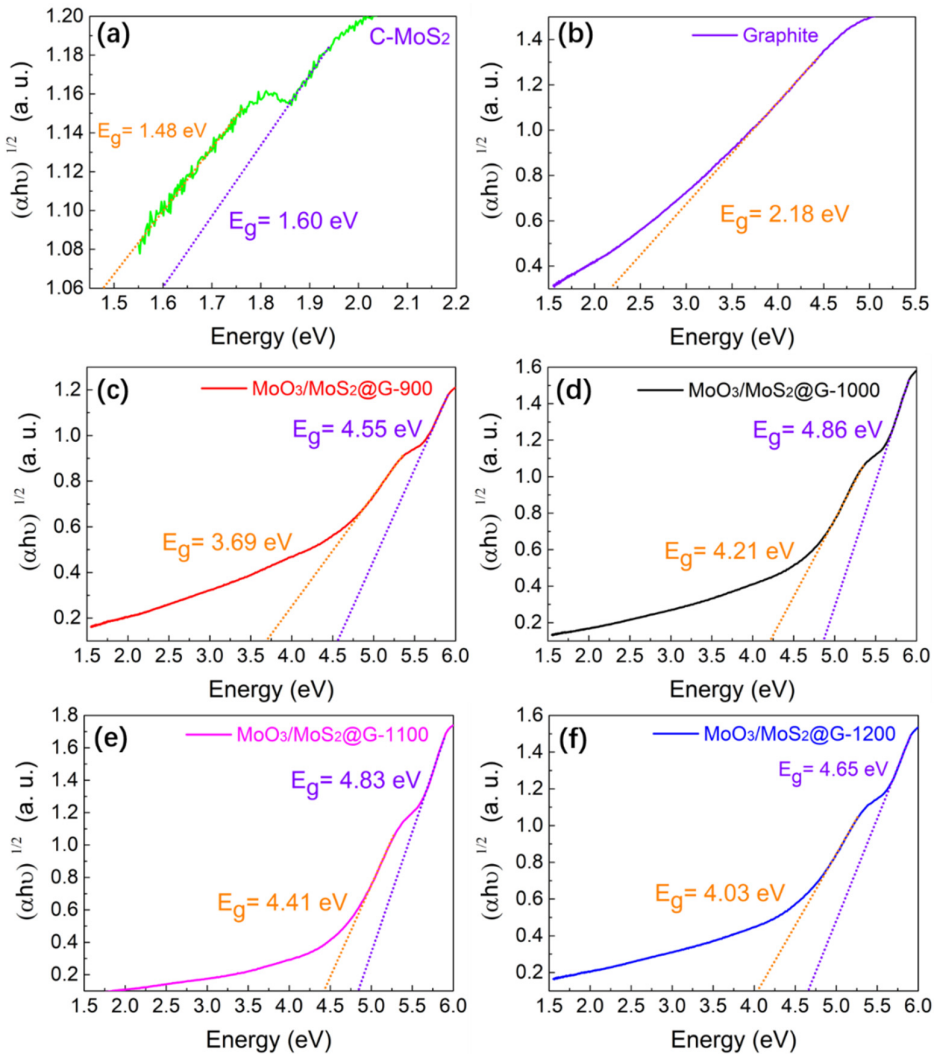

Figure S6. (αhν)$^{1/2}$ versus hν plots according to UV–vis spectra of various precursor materials and products obtained at various temperatures.

Table S2. Band gap values of various precursor materials and products obtained at various temperatures.

Sample	Eg1 (eV)	Eg2 (eV)
C-MoS_2	1.48	1.60
Graphite	2.18	
900 °C	3.69	4.55
1000 °C	4.21	4.86
1100 °C	4.41	4.83
1200 °C	4.03	4.65

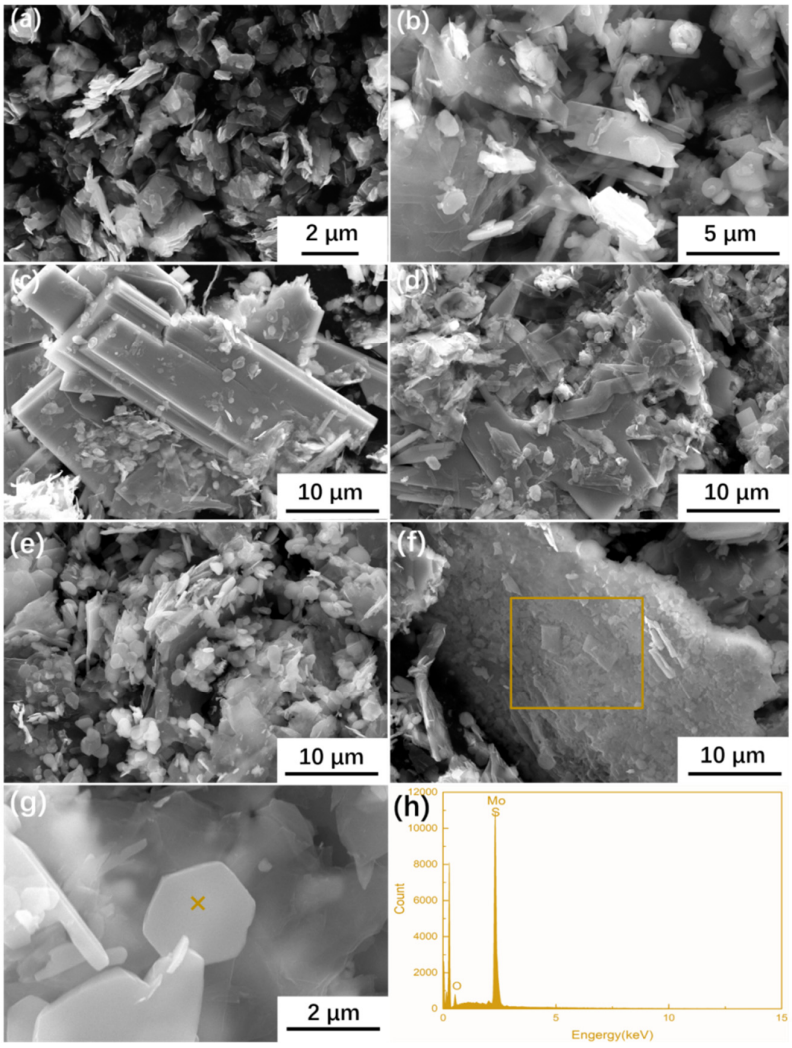

Figure S7. SEM image of (**a**) commercial MoS_2 and the samples prepared at (**b**) 900, (**c**) 1000, (**d**) 1100 , and (**e**-**f**) 1200 °C. (**g**) High magnification image taken on the sample prepared at 1200 °C, and (**h**) the EDS analysis recorded on hexagonal MoS_2 shown in (**g**).

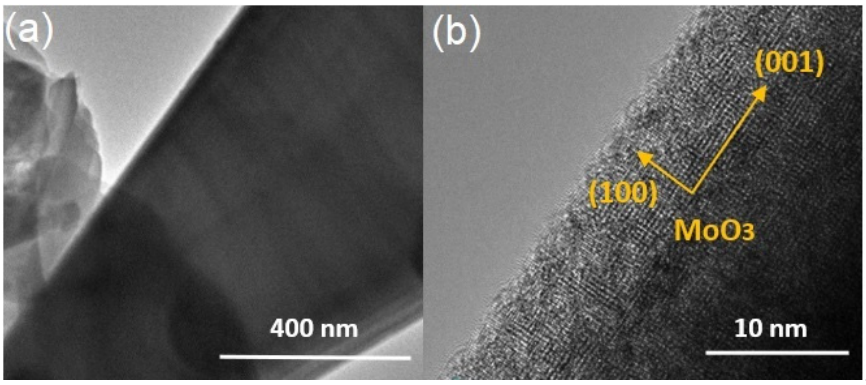

Figure S8. TEM micrographs of rod-like MoO_3 observed in MoO_3/MoS_2@G-900.

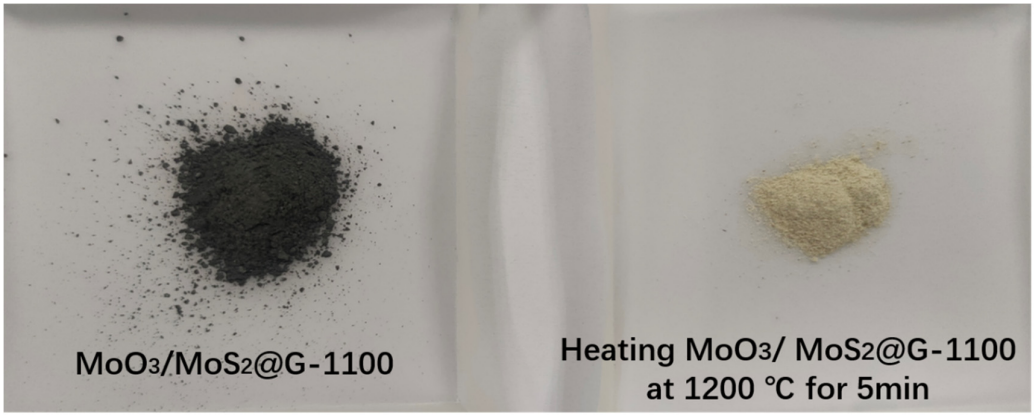

Figure S9. Appearance of MoO_3/MoS_2@G-1100, the same sample after heating at 1200 ℃ for 5 min.

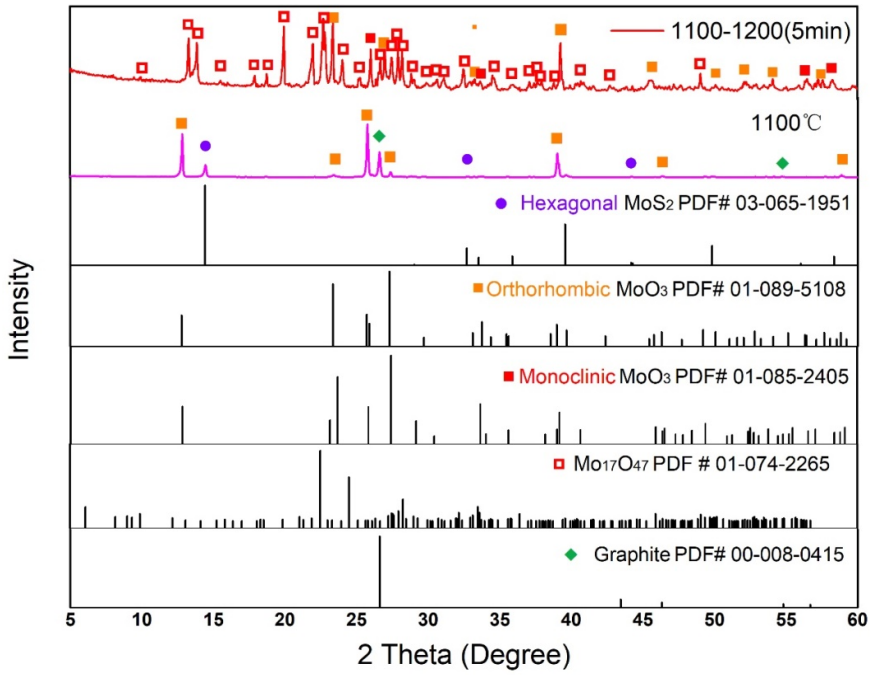

Figure S10. XRD patterns of MoO_3/MoS_2@G-1100 and the sample obtained by heating of MoO_3/MoS_2@G-1100 at 1200 ℃ for 5 min.

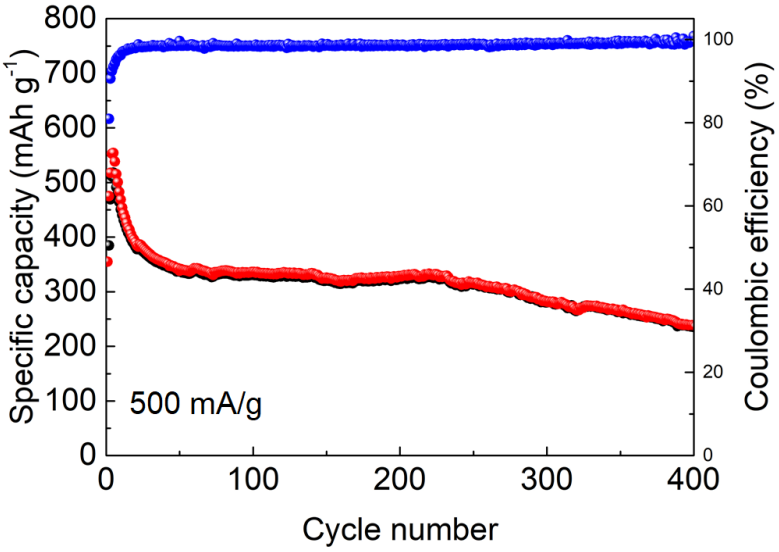

Figure S11. Cycling performance of MoO_3/MoS_2@G-1100 at 500 mA g^{-1}.

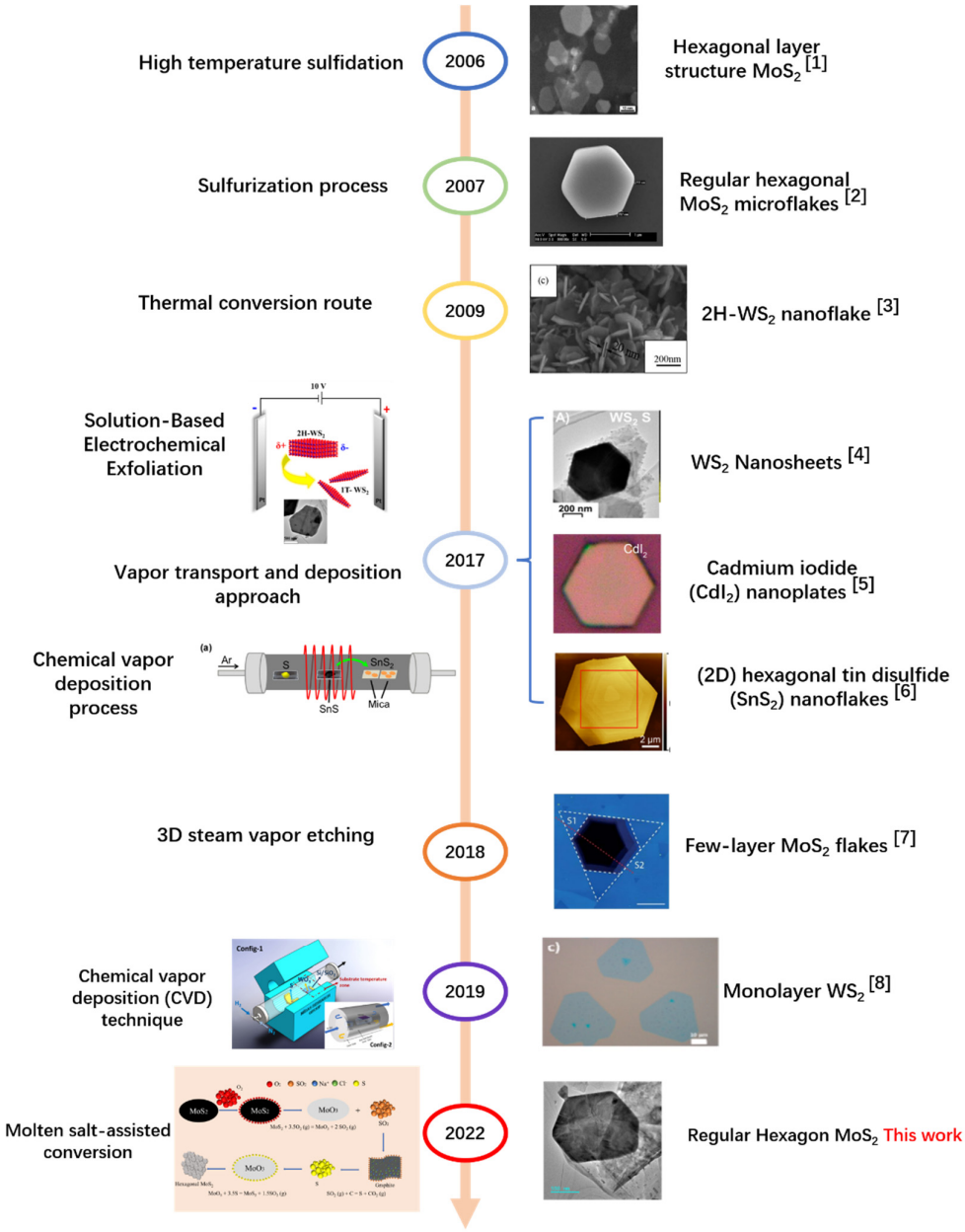

Figure S12. Summary of methods proposed for the preparation of hexagonally-shaped nanocrystals extracted from the literature.

Table S3. A comparison between precursor materials and the methods used for the preparation of hexagonal crystals extracted from the literature, with those produced in the current study.

Hexagonal crystal	Precursor materials	Preparation process
Hexagonal layer structure MoS_2 [31]	$(NH_4)_2MoS_4$, Ni(acetate)2	Sulfidation at 800 °C (6 h)
Hexagonal MoS_2 microflakes [32]	Pure Mo, S	Sulfurization at 750 °C (8 h), 350-110°C (4–10 h)
2H-WS_2 nanoflake [33]	Tungsten oxide rod, S	Thermal treatment at 750 °C (4 h)
WS_2 nanosheets [34]	WS_2, Na_2SO_4	Electrochemical exfoliation (48 h)
CdI_2 nanoplates [35]	WS_2, SiO_2/Si substrate, Ar	Vapor transport/deposition at 320 °C (40 min)
Hexagonal SnS_2 nanoflakes [36]	SnS, Ar	CVD at 200–550°C

		(36 min)
Few-layer MoS_2 flakes [77]	Si/SiO_2 substrate, MoS_2, Ar	Mechanical exfoliation and steam etching at 700 °C (30 min)
Monolayer WS_2 [78]	WO_3, Si/SiO_2 substrate, Ar	CVD at 100–180 °C
Hexagonal MoS_2 nanocrystals [This work]	MoS_2, natural graphite, NaCl	Molten salt-assisted conversion at 1100°C (20 min)